



In-situ, long-term operational stability of organic photovoltaics for off-grid applications in Africa

Christopher J.M. Emmott^{a,b}, Davide Moia^a, Philip Sandwell^{a,b}, Nicholas Ekins-Daukes^a, Markus Hösel^c, Lukas Lukoschek^d, Charith Amarasinghe^d, Frederik C. Krebs^c, Jenny Nelson^{a,b,*}

^a Department of Physics, Imperial College London, London SW7 2AZ, UK

^b Grantham Institute-Climate Change and the Environment, Imperial College London, SW7 2AZ, UK

^c Department of Energy Conversion and Storage, Technical University of Denmark, Frederiksborgvej 399, DK-4000 Roskilde, Denmark

^d MeshPower Limited, London SW7 2AZ, UK

ARTICLE INFO

Article history:

Received 30 September 2015

Received in revised form

8 January 2016

Accepted 28 January 2016

Available online 12 February 2016

Keywords:

Polymer solar cell modules

Outdoor testing in Africa

Failure mechanisms

Field testing

Off-grid application

ABSTRACT

This paper presents a field-trial of organic photovoltaic (OPV) technology used within a practical application for rural electrification in Rwanda. Fourteen, large area, flexible, ITO-free, roll-to-roll processed OPV modules, encapsulated with low-cost materials, were installed on corrugated steel roofs at two sites in a rural village in Southern Rwanda and subject to continuous monitoring. This field-trial exposed modules to very high levels of insolation, in particular in the UV, high temperatures and heavy rainfall. Results show that the modules exhibit practical lifetimes (to degrade by 20% of their initial capacity) of between 2½ and 5 months, a value 5–6 times lower than control modules kept both in the dark and outdoors in Roskilde, Denmark. Degradation was primarily the result of extensive delamination caused by failure of the non-UV stable encapsulation, which led to decay in the FF, V_{oc} and I_{sc} of the module.

© 2016 Elsevier B.V. All rights reserved.

1. Introduction

Organic photovoltaics (OPV), based on polymer:fullerene blends, offer the potential for a scalable technology, produced through rapid roll-to-roll (R2R) processes, which can provide very low costs [1] and minimal environmental impacts [2]. Such devices have been studied extensively within academia and industry in recent years, leading to large gains in the efficiency of this technology [3]. However, in order to realise its full potential, the lifetime of modules must be improved. Considerable work has been done on building a greater understanding of degradation mechanisms and predictions of OPV lifetime [4–6], but this work has largely focussed on very small devices (often less than 1 cm²), operating in laboratory conditions. Relatively few studies have looked at the stability of large area OPV modules under conditions which would be faced in practical applications [7–10]. This paper builds on the limited literature on the operation of large area modules within such practical applications.

One application where OPV technology may find a market is within off-grid photovoltaic systems powering small electrical loads. 1.3 billion people around the world have no access to

modern forms of energy (of whom 600 million live in Sub-Saharan Africa) [11], and largely rely on inefficient and hazardous fossil fuels such as kerosene lamps for lighting. These forms of lighting must be replaced with modern solutions, most importantly for respiratory health and fire safety reasons [12] but also for an improved light quality and decreased financial burden [13]. In addition, the use of kerosene lighting creates substantial greenhouse gas (GHG) emissions [14,15]. It has been estimated that worldwide use of kerosene lighting produces 189 MtCO_{2eq} annually (equal to the 28th highest emitting country) [16,17] and therefore represents a key application for GHG mitigation whilst also providing a host of ancillary benefits. Such an application requires a robust PV technology that can perform well under high temperatures, humid conditions, and dusty environments found in off-grid communities throughout Africa and Asia.

Studies on the outdoor degradation of OPV modules have, to date, focussed on Europe, and although a number of studies have reported performance in harsher conditions such as India, Israel and Ethiopia [9,18,19], these studies have looked at modules installed at laboratory sites rather than in real-world applications. The application of OPV technology in real-world conditions in Africa has been reported previously [20], although this study was limited by the difficulties of detailed data collection in such an environment.

* Corresponding author.

E-mail address: jenny.nelson@imperial.ac.uk (J. Nelson).

Here we present results of field trials of large area, roll-to-roll manufactured, ITO-free OPV technology using simple and low cost encapsulation operating under real-world conditions in rural Rwanda. This location presents an extreme environment where OPV may be used and thus the study provides an insight into the lifetime of OPV when used in such a real-world application. The sites in Rwanda demonstrate performance under challenging mounting conditions on uneven, corroded steel roofs, under high insolation, and heavy rainfall. This represents the first published report of the continuous monitoring of OPV technology in a practical application in a rural community in Africa.

1.1. Outdoor degradation of OPV modules

Analyses of the performance of OPV modules under outdoor conditions indicates the practical lifetime of OPV devices, although they do not always provide the most valuable insights for analysing specific degradation mechanisms. Such studies assess the module as a whole, rather than individual layers, and thus are equally an evaluation of the encapsulation as they are of the stability of the OPV materials themselves.

1.1.1. Metrics for assessing degradation

Stability analysis of OPV technology was standardised at the International summit on OPV stability (ISOS) [21]. These standards define what properties should be measured and how, as well as how to report results. These standards suggest that operational lifetime should be reported through the T_{80} metric, which quantifies the time for the performance of the device to fall by 20% from its initial, stabilised value. This metric therefore disregards any initial performance values prior to a period of rapid change in performance, such as due to a 'burn-in' period (for example improved performance after photo-annealing [22]). A second metric is also suggested, T_{s80} , which describes the time for the performance of the device to fall by 20% of that measured an interval T_s after fabrication.

1.1.2. Degradation of large area ITO-free OPV modules

This paper assesses the degradation of OPV modules based on an ITO-free architecture produced by the Technical University of Denmark (DTU). Modules used in this study (Fig. 1) have a device architecture which consists of: a Polyethylene terephthalate (PET) substrate; a cathode of high-conductivity poly(3,4-ethylenedioxythiophene) polystyrene sulphonate (PEDOT:PSS) combined with

a grid of silver paste (Ag-grid); a zinc oxide electron transport layer; an active layer of a blend of poly(3-hexylthiophene) (P3HT) and Phenyl-C61-butyric acid methyl ester (PCBM); a PEDOT:PSS hole transport layer; and topped by an Ag-grid anode. The devices are manufactured according to the *Infinity concept* which uses flexo-graphic printing, rotary screen printing and slot-die coating to deposit OPV materials on a PET substrate, through a roll-to-roll process, and is presented in detail elsewhere [23,24].

A number of studies have analysed degradation in very similar modules, which differ in size, encapsulation, and material used to contact the silver grid electrodes, which provide insights into the decay mechanisms seen in such modules [7–9,19,24–27]. It has been shown that the leading cause of degradation is due to ingress of atmospheric reactants from the edges of modules, and at the snap fastener (which is punched through the encapsulation). These reactants result in two principal degradation mechanisms being observed: photo-oxidation of the active layer, accelerated by oxygen, moisture and ozone formed by UV radiation; and delamination/degradation of the PEDOT:PSS layer due to moisture ingress which reduces conductivity and delaminates the weak bond between the PEDOT:PSS and active layer. Where photo-oxidation dominates, I_{sc} falls as the cells closest to the external contacts completely degrade, at which point they become resistors leading to a reduction in the V_{oc} and FF [9,25]. Degradation/delamination of PEDOT:PSS occurs more locally, allowing the V_{oc} to be maintained by small areas of all cells still being active, but reducing the FF. These mechanisms are greatly impacted by light levels, with active layer degradation being accelerated by high light levels, whilst water uptake by PEDOT:PSS is suppressed in light conditions [8].

Larger borders of the encapsulation around the module can provide improved edge sealing, greatly reducing degradation [9,28]. In addition, modules have shown a large spread in the level of degradation, which has been suggested to be due to the manual contacting of the modules leading to different levels of wear and tear before installation [9]. Similar issues around mechanical stability of the devices, and the need for careful handling has also been highlighted in a previous trial of DTU modules in Zambia [20], suggesting that careful handling of the modules can also reduce degradation.

2. Method

2.1. Organic PV modules

Modules used in this field trial (Fig. 1) consisted of a roll of serially connected cells produced by the *Infinity concept* (in rolls of several hundred metres, see above), cut into lengths of approximately 50 cm, containing 96 serially connected cells in order to deliver a V_{oc} of around 45 V, the maximum voltage which would ensure electrical safety of the system. These modules were encapsulated using thin polymer layers which comprise a UV-filter and hard-coating. A secondary double-side edge lamination using standard hotmelt office lamination pouches (80 μm) was applied to mechanically protect the edge from delamination and therefore oxygen/water ingress, creating a 1–2 cm wide edge, resulting in the ratio of active area to encapsulation area of 58% (the geometrical fill factor, GFF). Hotmelt office lamination pouches were chosen due to their low cost, which is likely to be a key criterion for the technology in this application. Contacts were made by punching a snap button through the encapsulation and substrate, and contacting with the large area of silver printed on the substrate. Contact wires were then snapped into the button and covered in epoxy resin to seal the connection and avoid ingress of water and oxygen at this point in the module.

All modules in the trial, including control modules kept in Denmark, had already been exposed to at least half a year outdoors in Denmark before being taken to Rwanda.

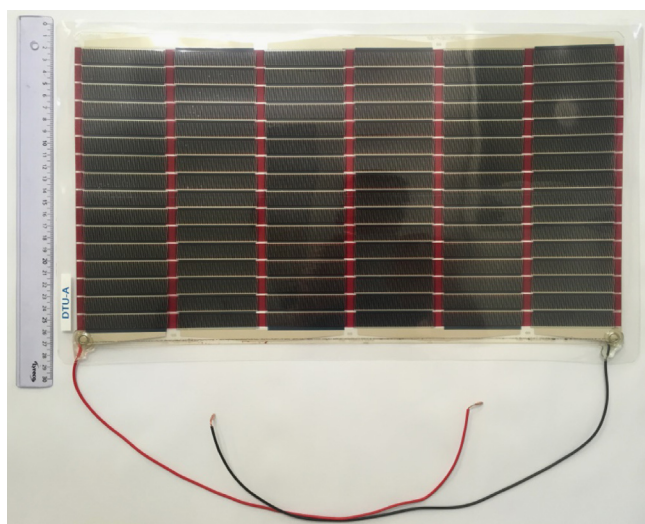


Fig. 1. Photograph of the OPV modules used in this study, showing both edge sealing and layout of electrical contacts in the module.

2.2. Installation in rural Rwanda

Collecting data from OPV modules in a remote community in Africa presents a major challenge. The company MeshPower operates solar powered mini-grid systems within Rwanda and have remote data logging capabilities to enable real-time monitoring of the systems, transferred to an online portal via GSM technology. This system allows electrical characteristics of the OPV modules to be continuously monitored through an automated system, and sent in real-time to an online portal. OPV modules were installed at two of MeshPower's sites in Kagano; a rural village in Bugusera District, Eastern Province, Rwanda, which lies two degrees south of the equator. The two sites lie a distance of approximately 300 m from each other. Seven modules were mounted at each site, on heavily corroded, corrugated steel roofs, at a tilt of around 8° and approximately oriented North, using heavy-duty VELCRO[®] which secured to the roof and modules with a water-proof adhesive. The edges of the modules were additionally secured using duct tape, to reduce vibrations caused by wind, which could accelerate de-lamination. The difficulties of transporting the modules to Kagano, and installing them on the roofs, resulted in significant mechanical stress on the modules, which could accelerate de-lamination. Fig. 2 shows the modules mounted at one site in Kagano. Alongside the OPV modules at each site, a small multi-crystalline silicon module was installed to provide a reference from which the performance of the OPV modules could be determined.

The sites in Rwanda were revisited 8 months into the trial, in May 2015, when a number of modules were collected for more detailed analysis of the state of degradation. In addition, remaining modules were cleaned of dirt that had accumulated over the previous 8 months.

2.3. Control modules

Control modules with exactly the same outline, pre-aging, edge sealing, and electrical contacts were also kept in Roskilde, Denmark, with one module kept at room temperature dark storage and a second outdoors on a solar tracker (attached with tape).

2.4. Environmental conditions

Kagano village in Rwanda lies at 1400 m elevation and, during the 9 months the systems were installed, experienced ambient



Fig. 2. A photograph of OPV modules at Kagano, totalling around $3.5 W_p$, alongside the small silicon reference module and larger silicon modules used for MeshPower's own system. Image courtesy of Philip Wood.

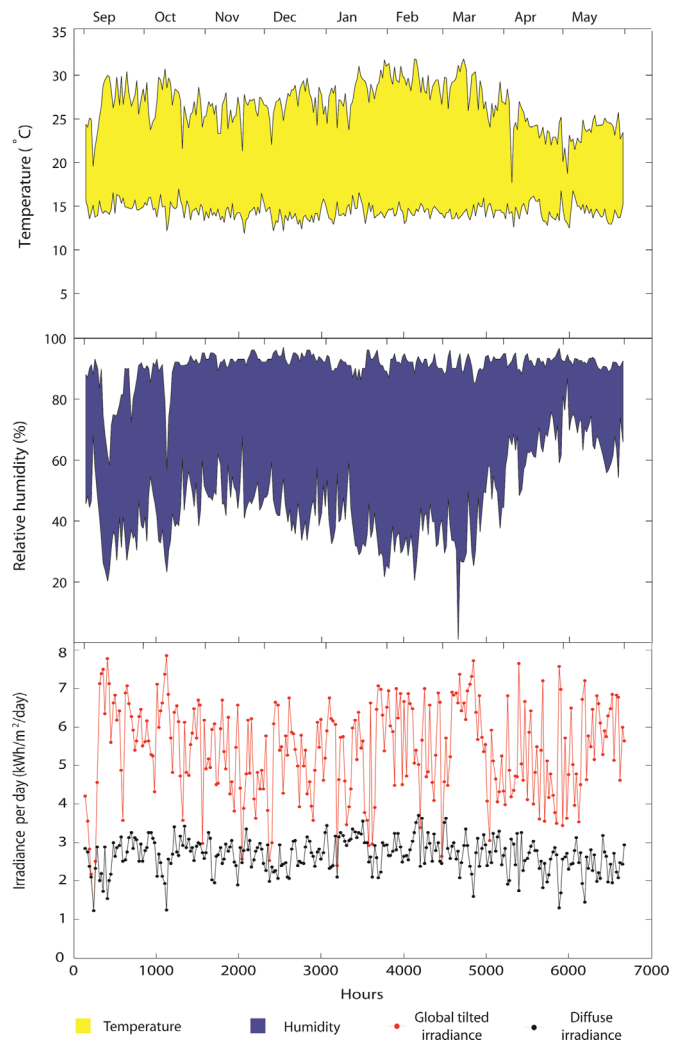


Fig. 3. Ambient temperature (top), humidity (middle) and global and diffuse irradiance (bottom) at the test site in Rwanda during the course of the trial.

temperature highs of $22\text{--}32^\circ\text{C}$, falling to $12\text{--}16^\circ\text{C}$ at night [29]. However, peak temperatures on the metal roofs where the PV modules were installed can be considerably higher. A temperature was measured on the back of one OPV module at over 70°C during the hottest part of the day. Humidity levels are between 70% and 95% [30]. By comparison, ambient temperatures experienced by the control module in Denmark showed mean highs of $2\text{--}22^\circ\text{C}$ across the testing period, occasionally reaching extremes of 32°C in the summer and -22°C in the winter, whilst humidity was in the range of 50–80% [31]. Fig. 3 shows the temperature, humidity and irradiance conditions in Rwanda throughout the testing period.

Irradiance at Kagano is very high, averaging $5.35 \text{ kWh/m}^2/\text{day}$, compared with around $3.4 \text{ kWh/m}^2/\text{day}$ in Northern Europe [32], and also has a considerably different spectrum compared with Europe. Insolation in Rwanda has a spectral distribution close to an air mass of 1.0 (AM 1.0) in contrast to AM 1.5 spectrum seen in Europe, resulting in greater UV radiation in Rwanda [33]. Moreover, the large difference between the diffuse and global irradiance (Fig. 3) shows that there is a high proportion of direct irradiance, suggesting frequent clear skies and hence high levels of UV irradiance. Over the 9 month trial, modules were exposed to a cumulative total (1st September 2014 to 30th May 2015) of

1645 kWh/m² [29]. By contrast, the control modules in Denmark received 720 kWh/m²¹ of solar irradiance over the same period.

The trial was conducted over two rainy seasons in Rwanda (October to November and March to May), which are interrupted by a drier season in December/January. During this time, thunderstorms accompanied by very heavy rain occur extremely frequently (although wind speeds remain very low throughout the year). This large amount of heavy rain exposes modules to high levels of moisture, but also places considerable mechanical stress on the modules, which could accelerate delamination.

The control module mounted outdoors in Denmark was first installed in summer 2014 and was exposed to considerable snow and rain during the winter season.

2.5. Data monitoring

Modules deployed in Rwanda were monitored according to the ISOS-O-2 protocol [21], with the exception of temperature, where only ambient measurements were possible, rather than operating cell temperatures as required by ISOS-O-2. Each of the 14 modules in Rwanda were independently monitored and held at maximum power point (MPP), with adjustments to the MPP every 30 s, and an IV curve taken every 30 min. Details of the electronics and methodology for determining the MPP are shown in the supplementary information. The relative irradiance was determined from the small crystalline silicon module mounted beside the OPV modules (see Fig. 1). In addition, satellite derived irradiance measurements provided by GeoModel Solar [29] were also used in order to support the measurements from the small silicon module. This satellite derived irradiance data has been shown to be accurate to within $\pm 8\%$ in the most extreme cases [34]. Temperature and humidity data was taken from modelled conditions based on satellite data, similarly provided by GeoModel Solar [29].

Control modules in Denmark were kept at open circuit and measured in the beginning (July 2014), after ca. half a year (January 2015), and after ca. one year (June 2015). The modules were measured under a solar simulator at 1 sun illumination and after 5–10 min of light soaking. Modules collected from Rwanda in May 2015 were returned to Denmark and measured under the solar simulator in June 2015.

All OPV modules had already experienced more than half a year outdoors in Denmark and both the OPV and small silicon modules exhibited some variation in their initial output. In order to normalise the data from these modules, the capacity of the small silicon module was first determined by comparing its average output over the first few days with that of a large (270 W_p) multi-crystalline silicon module from MeshPower's system, whose capacity was known precisely. The initial capacity of each of the individual OPV modules was then estimated by comparison of the module output with that of the small silicon module. These initial capacities were determined from the output of the OPV modules at measurement intervals when the small silicon module was producing within 1% of its capacity, averaged over the first 5 days of data being received (which was not until 8 days after the module were installed). The initial capacities were subsequently verified by normalising them against satellite insolation data.

Estimates of the capacity of the OPV modules are higher when determined by comparison to the output of the small silicon module than when estimated from simultaneous satellite derived insolation measurements. This is likely to be due, at least in part, to the difference in temperature coefficient between the technologies ($+0.007\%/K$ [7] and $-0.5\%/K$ [35] for OPV and multi-crystalline silicon respectively). This suggests a similar

systematic error is seen in measurements of degradation using the crystalline silicon module as a reference (i.e. Fig. 5).

3. Results

3.1. In-situ MPP and IV measurements

The initial capacities of the OPV modules are shown in Fig. 4. Specific energy production was determined for the first 2 months (before significant degradation occurred), and is shown in the supplementary info. Fig. 5 shows the evolution of the daily energy production, normalised to the initial value for each module and as a ratio of the small silicon energy production, for all the OPV modules in Rwanda over the course of 10 months. The daily yield was found from the integral of the MPP data. This shows a time to

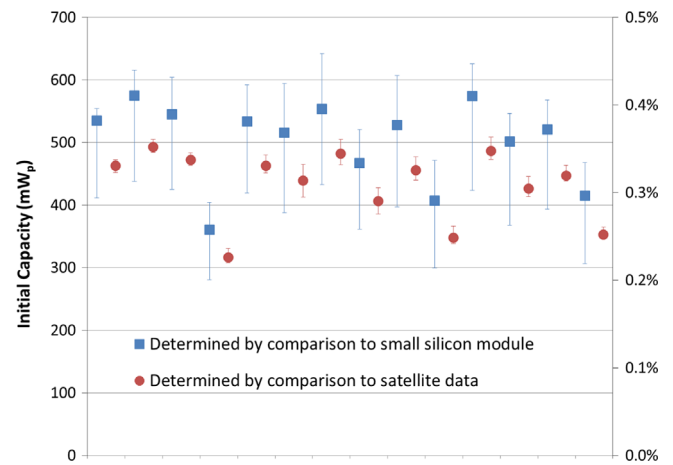


Fig. 4. Initial capacity and module efficiency of the OPV modules deployed in Rwanda. Kag1 indicates modules deployed at the first site in Kagano, and Kag2 the second, letters indicate different modules.

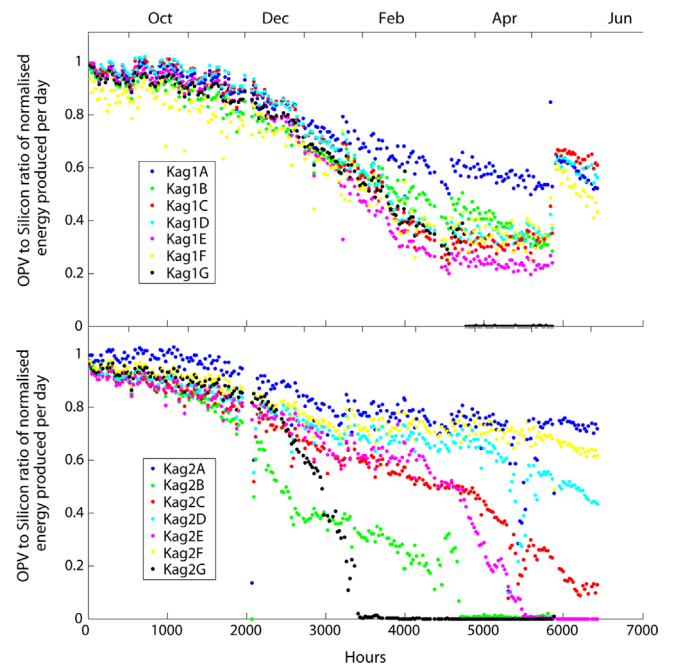


Fig. 5. Ratio of OPV to small silicon module of normalised daily energy production. The jump shown at 6000 h at the Kagano 1 site is due to cleaning which was done for all modules at both sites. At this time, some modules were also removed.

¹ Calculated from a pyrometer mounted beside the modules in Denmark.

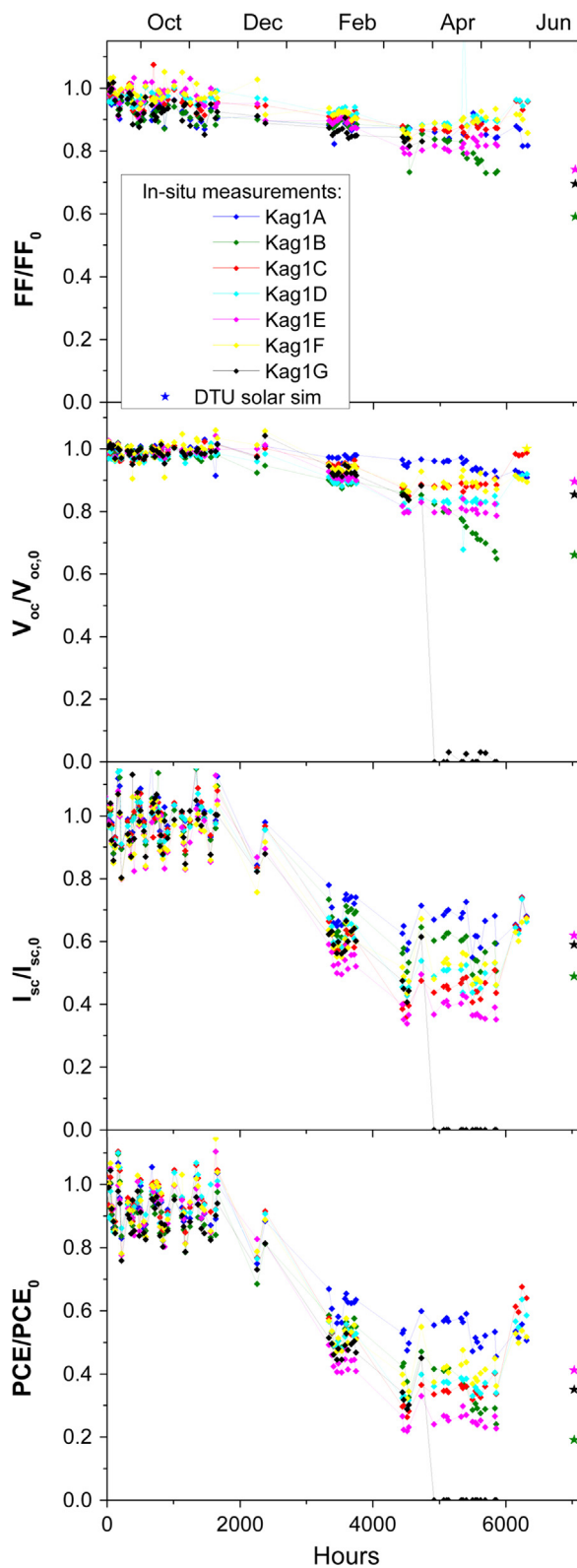


Fig. 6. Decay in photovoltaic performance characteristics for individual modules, normalised to initial values for modules at the Kagano 1 site. Data measured when insolation was within 1% of 1000 Wm^{-2} . Stars indicate measurements made in a solar simulator at DTU.

degrade by 20% from T_s (which is defined as 2 weeks after installation in Rwanda, which was when the initial values of the modules could be determined), T_{s80} , of 1700–3000 h.

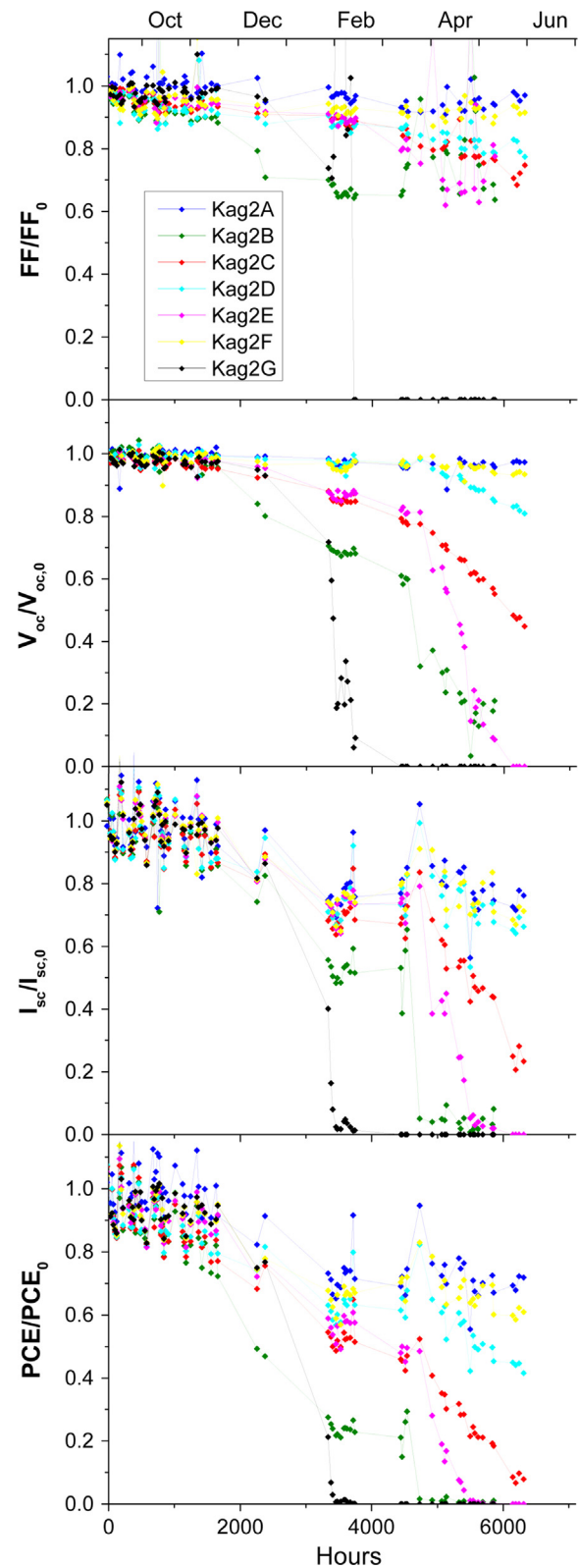


Fig. 7. Decay in photovoltaic performance characteristics for individual modules, normalised to initial values for modules at the Kagano 2 site. Data measured when insolation was within 1% of 1000 Wm^{-2} . Note that there are no data points from measurements with the solar simulator at DTU as all the modules brought back to Denmark (Kag2B, Kag2E and Kag2G) were completely degraded and so no IV curve could be made.

Along with the range in T_{s80} , Fig. 5 also shows a variety of decay paths. Four of the 14 modules showed complete failure within the 9 months of the trial, however, the time to failure varied

considerably. During the return trip in May 2015, the cable connected to Kag1G was found to be broken, perhaps explaining the sudden drop in this module's performance, and suggesting that in fact only 3 out of the 14 modules failed.

For all other modules, with the exception of Kag2C, the modules exhibit a plateau in the degradation path at approximately 4000 h, where degradation appears to slow after degrading by 30–70%. This occurs at approximately 4500 h at Kagano 1 site, and at 3250 h at Kagano 2. This difference in the timing and level of degradation of the plateau at the different sites may be the result of increased soiling at Kagano 1, which was the result of a fire near the roof of the Kagano 1 site.

The modules were cleaned at the start of May 2015. This can be clearly seen in Fig. 5 in the sudden jump in values seen in early May at the Kagano 1 site. Modules at the Kagano 1 site were much dirtier than those at the Kagano 2 site, as mentioned previously. Modules at the Kagano 2 site show little change in performance after cleaning suggesting that normal levels of dirt have limited impact on the performance.

Figs. 6 and 7 show the degradation in the individual parameters of the OPV modules installed in Rwanda, and largely agree with the decay trend shown in Fig. 5. These values were taken from *IV* curves measured at times of the day when insolation was within $\pm 1\%$ of 1000 W/m^2 , as determined by the satellite data. These graphs therefore give a good indication of the timing of the rainy season (as during cloudy days there are no data points).

Within the 7 modules at the Kagano 1 site (Fig. 6), the decay paths show that the principal degradation occurs in the I_{sc} , which falls by 30–70%, after a stable period of around 2000 h, before again stabilising after 4000 h (Fig. 6). Meanwhile, the V_{oc} and FF of all modules at this site show approximately linear degradation by 10–30% by the end of the trial. The Kagano 2 site (Fig. 7) shows much more scattered results, with a number of modules showing severe and rapid decay in V_{oc} at the same time as rapid decay in the I_{sc} .

3.2. Control modules

Fig. 8 shows the results from occasional *IV* curves taken under a solar simulator of the control modules kept in Denmark.

3.3. Photographic analysis

Figs. 9 and 10 show backlit photographs of the OPV modules brought back from Rwanda. They clearly show a number of defects in the modules as a result of 8 months of outdoor exposure in Rwanda. Modules Kag1B, Kag2B, Kag2E and Kag2G all show severe delamination of the encapsulation which has allowed the ingress of water, air, and even dirt, into the device. Moreover, Kag1G, Kag2B and Kag2G clearly show areas where the polymer has bleached or degraded, such that areas of the device now appear transparent. Photographs of the modules in-situ are shown in the supplementary information. These indicate that, additionally, modules Kag1C, Kag2C and Kag2D have significant areas which are delaminated. However, since these images are not backlit, bleaching could not be observed.

3.4. Characterisation of sub-modules

By measuring the performance of different areas of the module, the performance of areas where delamination occurred can be compared with areas where this is not visible. Such measurements were made by piercing the encapsulation and connecting electrodes at either end of a 16-cell submodule (seen as one column of

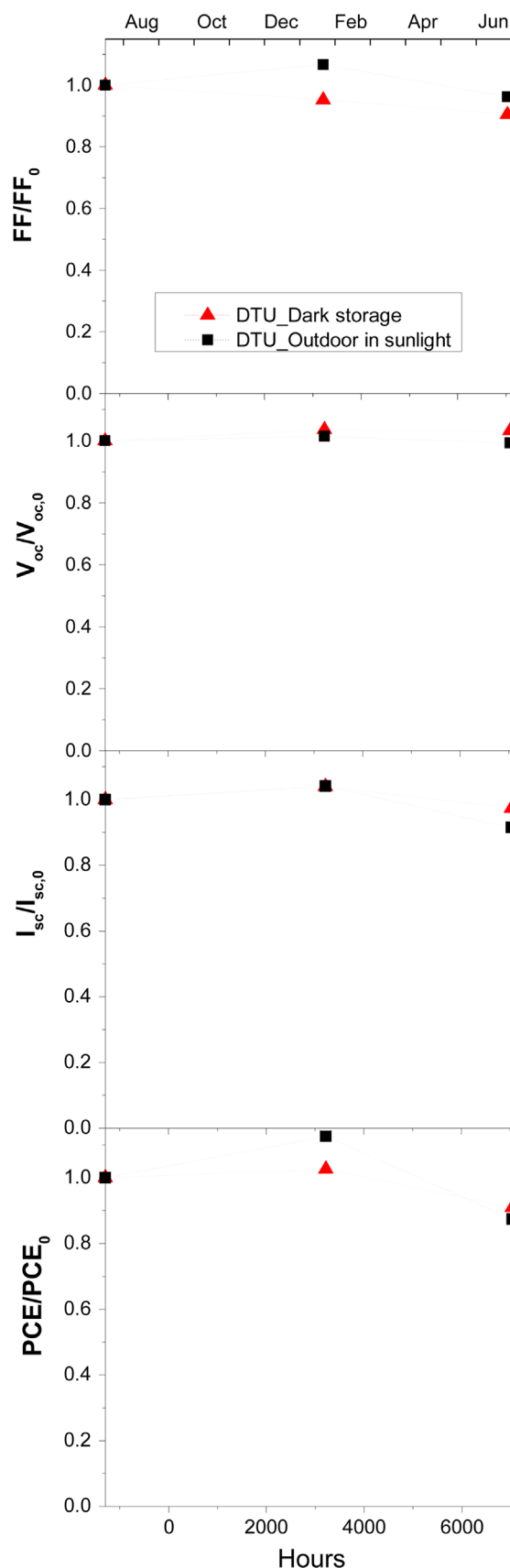


Fig. 8. Performance characteristics of control modules kept at DTU normalised to values when first measured. Zero on the x-axis indicates T_s , the starting point of measurements for the modules in Rwanda.

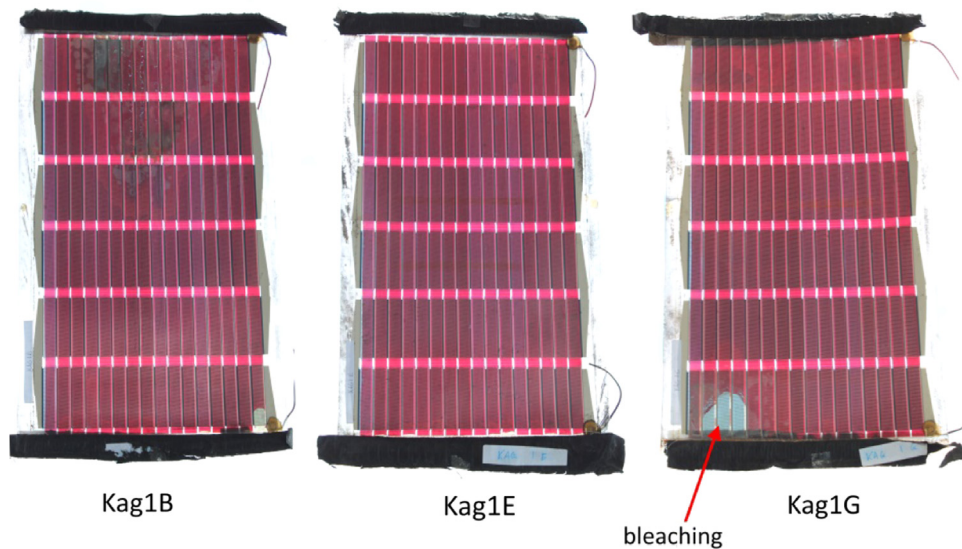


Fig. 9. Backlit photographs of OPV modules from Kagano 1 site brought back to Denmark from Rwanda.

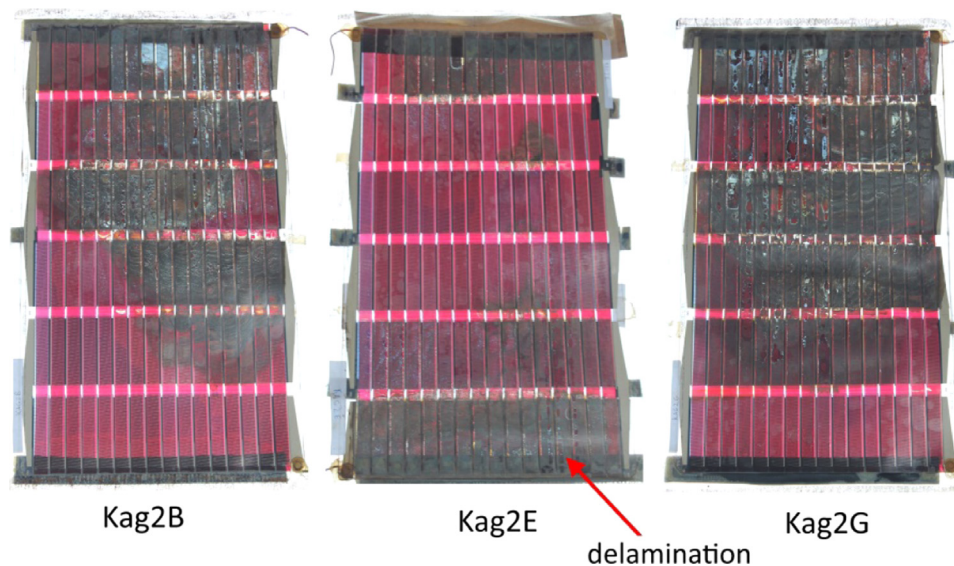


Fig. 10. Backlit photographs of OPV modules from Kagano 2 site brought back to Denmark from Rwanda.

serially connected cells in Fig. 1), and running a voltage sweep of the submodule. This allowed for insights into how the performance may have been impacted if more effective encapsulation, to reduce water and oxygen ingress, was used. Fig. 11 shows the performance characteristics of the submodules for each of the modules returned to Denmark from the Kagano 1 site. No data was extracted from submodules which did not produce an IV curve, although in some cases these still seem to contribute to the V_{oc} of the module. Modules from the Kagano 2 site were too degraded to extract any submodule performance data. The corresponding IV curves are shown in the supplementary information.

4. Discussion

4.1. OPV lifetime under harsh environmental conditions

The T_{s80} lifetimes for all modules are shown in Fig. 12 and their values range between 2 and 4½ months. In the longer term there is

a much larger spread in the level of degradation. At the Kagano 2 site, four of the seven modules see rapid and severe degradation after between 3 and 7 months.

Figs. 5 and 6 show a significant increase in the performance of modules at the Kagano 1 site after cleaning. However, the performance rapidly decays again, suggesting that the soiling occurs very quickly. This suggests that at the time when data started to be collected, T_s , two weeks after first being installed, the modules were likely to be already heavily soiled and therefore the observed reduction in performance over the trial is due to degradation alone.

T_{s80} lifetimes provide an indication of the lifetime from a practical viewpoint, as being the useful lifetime for a consumer using OPV. This takes as the starting point a value of the power output after the modules have been in place for two weeks, which was necessitated by the experimental set-up but also accounts for any “burn-in” or rapid dirtying of the modules. This means that these lifetimes could safely be assumed to be 2 weeks longer than the values given here, hence suggesting a practical lifetime for the technology in this application of 2½ to 5 months. Moreover, these

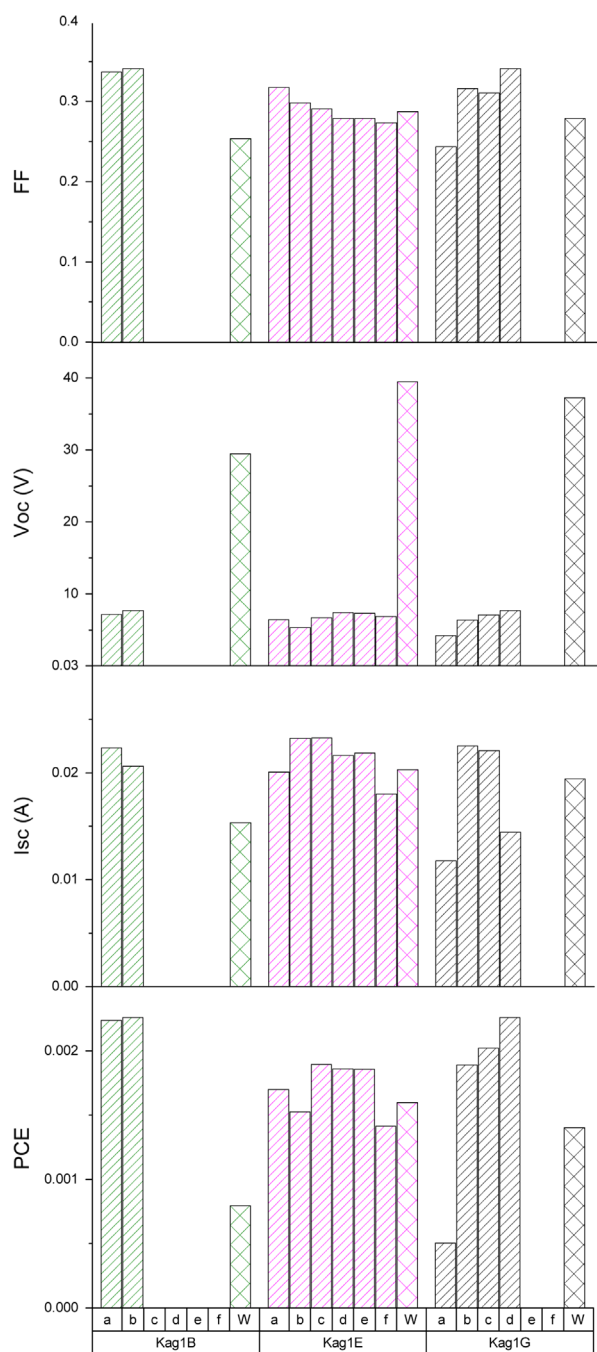


Fig. 11. Performance characteristics of 16 cell submodules in three modules from the Kagano 1 site. The labels a, b, c, d, e and f indicate different submodules; W indicates characteristics of the whole module.

modules had previously been outside in Denmark for more than 6 months, suggesting that this is a conservative assessment of the total energy which could be generated by the modules over their entire lifetime.

For the control modules, estimates from a linear fit of the decay curves shown in Fig. 8 indicate lifetimes of between 24 and 33 months (consistent with a similar previous study [8]). This is 5 or 6 times what was achieved within the practical application in Rwanda. This difference may be the result of higher temperatures and higher insolation levels (particularly in the UV, due to the AM 1.0 spectrum experienced in Rwanda) or higher mechanical stress on the modules (which occurred during transport and installation in Rwanda).

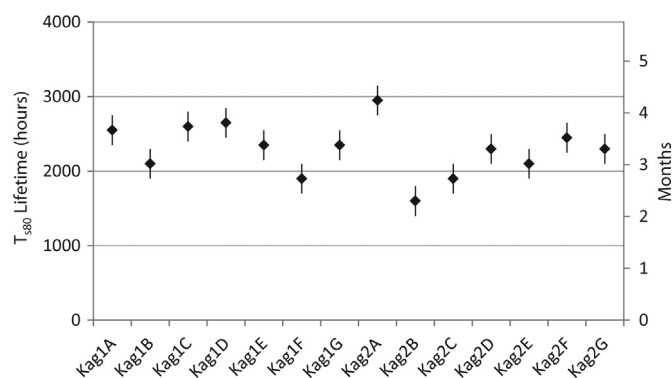


Fig. 12. Lifetimes of OPV modules in Rwanda.

4.2. Mechanisms of degradation

4.2.1. Degradation of encapsulation

Inspection of the modules in Rwanda show that the hotmelt office lamination foil became brittle; most likely due to the high UV and high temperatures experienced in Rwanda [36]. This led to failure of the encapsulation in a number of the modules, allowing extensive ingress of atmospheric reactants into the device. By contrast, the encapsulation of the control modules remained soft and flexible, and in these cases, no delamination can be observed (see [Supplementary information](#)).

Degradation and delamination of the encapsulation allows significant ingress of atmospheric reactants into the device. Such reactants have been shown to lead to prominent interfacial and contact decay through oxidation of the contacts and delamination/degradation of the PEDOT:PSS, leading to decay of V_{oc} and FF [9]. Figs. 6, 7, 9 and 10 corroborate this, showing that a decline in V_{oc} and FF is most pronounced in modules with greater levels of visible delamination. Moreover, these results show that modules with very extensive visible delamination (e.g. Kag2B, Kag2C, Kag2E and Kag2G) experience abrupt decay in V_{oc} , suggesting that more severe interfacial and contact decay eventually acts to degrade the V_{oc} completely.

4.2.2. Impact of high UV and temperature

A drop in I_{sc} alone could be the result of local photo-oxidation in the presence of water and/or oxygen and UV radiation or doping of the active layer by oxygen which results in deeper trap states and lower mobility [8,9,37,38]. Most modules, regardless of the level of visible delamination, follow a similar trend in I_{sc} , suggesting that delamination has less of an impact on I_{sc} than on V_{oc} or FF. This suggests that the presence of large amounts atmospheric reactants is not the principal driver of the decay of I_{sc} , and suggests that I_{sc} decay is more strongly driven by the high levels of UV and high temperatures found in Rwanda. This is supported by the results of the control modules, which experienced lower UV and temperature levels (Fig. 11). Moreover, Figs. 6 and 7 show that the I_{sc} stops decaying after around 4000 h. This suggests that this degradation mechanism has a limit and does not completely degrade the modules over the course of the trial. However, this only holds true up to a certain level of delamination, beyond which rapid decay in I_{sc} is observed, as seen in some of the modules at the Kagano 2 site.

Figs. 9 and 10 show areas of delamination seemingly covering complete cells (e.g. centre top of Kag1B). This would be expected to completely degrade the cell, and hence create a disconnection the module. However, the module continues to generate power regardless of this, suggesting that despite severe delamination, there is still at least a small area of the cell remaining functional, or at least not acting as a disconnect. This demonstrates the

robustness of the modules, showing that they still function despite severe levels of delamination and hence exposure to atmospheric reactants. A photograph of module Kag2B, taken in February 2015, further corroborates this point (see [Supplementary information](#)).

4.2.3. Other factors

This trial shows that delamination is a significant cause of degradation of the modules, and is the sole cause of catastrophic failure. The care taken when handling the modules seems to impact the level of delamination, as has previously been observed [20]. This experiment was not designed to assess this and so no controlled, side-by-side comparison was made of roughly vs. carefully handled modules. However, modules at the Kagano 2 site were more roughly handled due to this roof being more difficult to access. These modules show much higher levels of delamination (see [Fig. 10](#) and [Supplementary information](#)). In addition, the control modules which were not taken to Rwanda, and therefore experienced much less mechanical stress also show no delamination. This suggests that rough handling increases chance of rapid degradation through delamination of the encapsulation. However, the difference between modules at the Kagano 1 and Kagano 2 sites could also be due to levels of dirt (modules at Kagano 1 were much dirtier, as mentioned previously) reducing the irradiance and levels of UV received, which may have reduced the degree of delamination.

4.3. Application of OPV in rural Africa

The process of installing OPV modules in rural Rwanda gave some insights into the applicability of OPV for this application. The low efficiency of the OPV modules (around 0.35% over the total area) means that large areas would be needed. Off-grid solar lighting systems often require only a few Watts of PV capacity, and so low efficiency may not present a barrier to the technology in terms of available roof space (see [Fig. 2](#)). The modules used in this study took a long time to install due to the relatively small size of the individual modules, and so larger single modules would be needed for simpler installation. However, this could present a challenge for careful handling, which is needed to reduce the likelihood of delamination, suggesting that higher efficiencies and/or more robust encapsulation is needed to improve reliability of modules. For the capacities required for an off-grid lighting system, OPV presents a more challenging installation process than crystalline silicon technology, due to its much lower efficiency.

This study shows OPV lifetimes in a rural African application of 2½ to 5 months. Such a lifetime would mean that the OPV modules would need to be replaced regularly over the lifetime of the other system components (battery, electronics, etc.), which often have design lives of 2–5 years. This would require more established distribution channels to enable replacements to be delivered, which may increase the costs of such a system compared with using more mature PV technology, but could also increase reliability, due to the need for the supplier to maintain regular contact with the consumer of the off-grid lighting product. The short lifetimes would also require OPV to be lower cost than mature technology in order to be competitive, however, if this were the case, then the lower value of OPV modules could reduce theft, which is increasingly becoming an issue for off-grid solar lighting products [39].

5. Conclusion

This study presents the first published results of continuous monitoring of OPV modules installed within a practical application; for powering small electrical loads (LED lighting, phone

charging, etc.) in rural Sub-Saharan Africa. Fourteen ITO-free organic photovoltaic modules, encapsulated using low cost materials and processing techniques, were installed on corrugated steel roofs in a village in Southern Rwanda and subject to real-time monitoring of performance characteristics. Results show that such modules exhibit a practical lifetime for use in this application (taken as degrading by 20% of their initial capacity) of between 2½ and 5 months. This is 5 to 6 times shorter than lifetimes exhibited by control modules kept both in the dark and under outdoor conditions in Denmark.

The primary cause of degradation was seen to result from degradation of the encapsulation, which allowed extensive ingress of atmospheric reactants. The failure of the encapsulation was also likely exacerbated by the rough handling of the modules which was necessitated by the difficult installation conditions experienced in Rwanda. However, modules which showed little delamination still exhibited decay in the I_{sc} , suggesting that even with improved encapsulation, the high temperatures, insolation and UV levels found in Rwanda will remain a challenge for OPV if used in this application. This suggests that in order to reach lifetimes in a practical application in Rwanda that are comparable to those seen in Europe, improvements to encapsulation, UV filtration, and mechanical robustness are required. We finally also note that dust accumulation on the surface of the solar cells is a particular challenge that might be more prominent for solar cells with a plastic front face as compared to traditional solar cells that employ a glass front face.

Acknowledgements

This work was supported by Climate-KIC and the European Commission's CHEETAH Project (FP7-Energy-2013- Grant no. 609788). The authors would like to thank Jean Marie Vianney Umizerwa, Hassan Souleyman, Longin Sebahizi and Phillip Wood for their support during installation in Rwanda. DM is grateful for EPSRC fellowship EP/J002305/1 and support from the Energy Futures Lab, Imperial College London. CJME and PS acknowledge support from the Grantham Institute – Climate Change and the Environment and Climate-KIC through PhD studentships. JN acknowledges support from the Royal Society through a Wolfson Merit Award.

Appendix A. Supplementary material

Supplementary data associated with this article can be found in the online version at <http://dx.doi.org/10.1016/j.solmat.2016.01.036>.

References

- [1] F. Machui, M. Hösel, N. Li, G.D. Spyropoulos, T. Ameri, R.R. Søndergaard, et al., Cost analysis of roll-to-roll fabricated ITO free single and tandem organic solar modules based on data from manufacture, *Energy Environ. Sci.* 7 (2014) 2792–2802, <http://dx.doi.org/10.1039/C4EE01222D>.
- [2] N. Espinosa, M. Hösel, D. Angmo, F.C. Krebs, Solar cells with one-day energy payback for the factories of the future, *Energy Environ. Sci.* 5 (2012) 5117–5132, <http://dx.doi.org/10.1039/c1ee02728j>.
- [3] M. Jørgensen, J.E. Carlé, R.R. Søndergaard, M. Lauritzen, N.A. Dagnæs-hansen, S.L. Byskov, et al., The state of organic solar cells – a meta analysis, *Sol. Energy Mater. Sol. Cells* 119 (2013) 84–93, <http://dx.doi.org/10.1016/j.solmat.2013.05.034>.
- [4] M. Jørgensen, K. Norrman, S. A. Gevorgyan, T. Tromholt, B. Andreasen, F. C. Krebs, Stability of polymer solar cells, *Adv. Mater.* 24 (2012) 580–612, <http://dx.doi.org/10.1002/adma.201104187>.

- [5] M. Jørgensen, K. Norrman, F.C. Krebs, Stability/degradation of polymer solar cells, *Sol. Energy Mater. Sol. Cells* 92 (2008) 686–714, <http://dx.doi.org/10.1016/j.solmat.2008.01.005>.
- [6] S.A. Gevorgyan, Lifetime of organic photovoltaics: status and predictions, *Adv. Energy Mater.* (2015), <http://dx.doi.org/10.1002/aenm.201501208>.
- [7] N. Bristow, J. Kettle, Outdoor performance of organic photovoltaics: diurnal analysis, dependence on temperature, irradiance, and degradation, *J. Renew. Sustain. Energy* 7 (2015) 013111, <http://dx.doi.org/10.1063/1.4906915>.
- [8] D. Angmo, F.C. Krebs, Over 2 years of outdoor operational and storage stability of ITO-free, fully roll-to-roll fabricated polymer solar cell modules, *Energy Technol.* 3 (2015) 774–783, <http://dx.doi.org/10.1002/ente.201500086>.
- [9] D. Angmo, P.M. Sommeling, R. Gupta, M. Hösel, S.A. Gevorgyan, J.M. Kroon, et al., Outdoor operational stability of indium-free flexible polymer solar modules over 1 year studied in India, Holland, and Denmark, *Adv. Eng. Mater.* 16 (2014) 976–987, <http://dx.doi.org/10.1002/adem.201400002>.
- [10] F. Yan, J. Noble, J. Peltola, S. Wicks, S. Balasubramanian, Semitransparent OPV modules pass environmental chamber test requirements, *Sol. Energy Mater. Sol. Cells* 114 (2013) 214–218, <http://dx.doi.org/10.1016/j.solmat.2012.09.031>.
- [11] International Energy Agency, *World Energy Outlook 2014*, Paris, France, 2014.
- [12] E. Mills, *Light for Life: Identifying and Reducing the Health and Safety Impacts of Fuel-based Lighting*, Geneva, Switzerland, 2014.
- [13] R. Bacon, S. Bhattacharya, M. Kojima, Expenditure of Low-Income Households on Energy: Evidence from Africa and Asia, Washington, D.C., United States, 2010.
- [14] S. Mahapatra, H.N. Chanakya, S. Dasappa, Evaluation of various energy devices for domestic lighting in India: technology, economics and CO₂ emissions, *Energy Sustain. Dev.* 13 (2009) 271–279, <http://dx.doi.org/10.1016/j.esd.2009.10.005>.
- [15] N.L. Lam, Y. Chen, C. Weyant, C. Venkataraman, P. Sadavarte, M.A. Johnson, et al., Household light makes global heat: high black carbon emissions from kerosene wick lamps, *Environ. Sci. Technol.* 46 (2012) 13531–13538, <http://dx.doi.org/10.1021/es302697h>.
- [16] E. Mills, The specter of fuel-based lighting, *Science* 308 (2005) 1263–1264, <http://dx.doi.org/10.1126/science.1113090>.
- [17] The World Bank, World Bank Open Data, (<http://data.worldbank.org/>), 2015 (accessed 21.04.15).
- [18] E.A. Katz, S.A. Gevorgyan, M.S. Orynbayev, F.C. Krebs, Out-door testing and long-term stability of plastic solar cells, *Eur. Phys. J. Appl. Phys.* 36 (2006) 307–311, <http://dx.doi.org/10.1051/epjap>.
- [19] M.V. Madsen, S.A. Gevorgyan, R. Pacios, J. Ajuria, I. Etxebarria, J. Kettle, et al., Worldwide outdoor round robin study of organic photovoltaic devices and modules, *Sol. Energy Mater. Sol. Cells* 130 (2014) 281–290, <http://dx.doi.org/10.1016/j.solmat.2014.07.021>.
- [20] F.C. Krebs, T.D. Nielsen, J. Fyenbo, M. Wadstrøm, M.S. Pedersen, Manufacture, integration and demonstration of polymer solar cells in a lamp for the “Lighting Africa” initiative, *Energy Environ. Sci.* 3 (2010) 512, <http://dx.doi.org/10.1039/b918441d>.
- [21] M.O. Reese, S.A. Gevorgyan, M. Jørgensen, E. Bundgaard, S.R. Kurtz, D.S. Ginley, et al., Consensus stability testing protocols for organic photovoltaic materials and devices, *Sol. Energy Mater. Sol. Cells* 95 (2011) 1253–1267, <http://dx.doi.org/10.1016/j.solmat.2011.01.036>.
- [22] M.R. Lilliedal, A.J. Medford, M.V. Madsen, K. Norrman, F.C. Krebs, The effect of post-processing treatments on inflection points in current-voltage curves of roll-to-roll processed polymer photovoltaics, *Sol. Energy Mater. Sol. Cells* 94 (2010) 2018–2031, <http://dx.doi.org/10.1016/j.solmat.2010.06.007>.
- [23] F.C. Krebs, N. Espinosa, M. Hösel, R.R. Søndergaard, M. Jørgensen, 25th anniversary article: rise to power – OPV-based solar parks, *Adv. Mater.* 26 (2014) 29–39, <http://dx.doi.org/10.1002/adma.201302031>.
- [24] P. Sommer-Larsen, M. Jørgensen, R.R. Søndergaard, M. Hösel, F.C. Krebs, It is all in the pattern-high-efficiency power extraction from polymer solar cells through high-voltage serial connection, *Energy Technol.* 1 (2013) 15–19, <http://dx.doi.org/10.1002/ente.201200055>.
- [25] D. Angmo, S.A. Gevorgyan, T.T. Larsen-Olsen, R.R. Søndergaard, M. Hösel, M. Jørgensen, et al., Scalability and stability of very thin, roll-to-roll processed, large area, indium-tin-oxide free polymer solar cell modules, *Org. Electron.* 14 (2013) 984–994, <http://dx.doi.org/10.1016/j.orgel.2012.12.033>.
- [26] B. Roth, G.A. dos Reis Benatto, M. Corazza, R.R. Søndergaard, S.A. Gevorgyan, M. Jørgensen, et al., The critical choice of PEDOT:PSS additives for long term stability of roll-to-roll processed OPVs, *Adv. Energy Mater.* (2015) 1401912, <http://dx.doi.org/10.1002/aenm.201401912>.
- [27] M. Hösel, R.R. Søndergaard, M. Jørgensen, F.C. Krebs, Failure modes and fast repair procedures in high voltage organic solar cell installations, *Adv. Energy Mater.* 4 (2014) 1301625, <http://dx.doi.org/10.1002/aenm.201301625>.
- [28] D.M. Tanenbaum, H.F. Dam, R. Rösch, M. Jørgensen, H. Hoppe, F.C. Krebs, Edge sealing for low cost stability enhancement of roll-to-roll processed flexible polymer solar cell modules, *Sol. Energy Mater. Sol. Cells* 97 (2012) 157–163, <http://dx.doi.org/10.1016/j.solmat.2011.09.064>.
- [29] GeoModel Solar s.r.o., Solar GIS, (n.d.), (<http://solargis.info>), 2012 (accessed 23.03.12).
- [30] WeatherSpark, Kigali International Airport, (<https://weatherspark.com/#!dashboard;ws=29294;t0=1/1;t1=12/31;graphs=temperature:1>), 2015 (accessed 28.03.15).
- [31] WeatherSpark, Roskilde Airport, (<https://weatherspark.com/#!dashboard;ws=29294;t0=1/1;t1=12/31;graphs=temperature:1>), 2015 (accessed 28.04.2015).
- [32] European Commission Joint Research Centre, Photovoltaic Geographical Information System, (<http://re.jrc.ec.europa.eu/pvgis/apps4/pvest.php>), 2013 (accessed 04.04.13).
- [33] R.J. Matson, K.A. Emery, R.E. Bird, Terrestrial solar spectra, solar simulation and solar cell short-circuit current calibration: a review, *Sol. Cells* 11 (1984) 105–145, [http://dx.doi.org/10.1016/0379-6787\(84\)90022-X](http://dx.doi.org/10.1016/0379-6787(84)90022-X).
- [34] GeoModel Solar s.r.o., Accuracy of Solar GIS data, (n.d.), (<http://solargis.info/doc/accuracy>), 2015 (accessed 18.12.15).
- [35] BBOX Ltd., BBOX BB7 Kit Datasheet, (<http://www.bbox.co.uk/our-products/>), 2012.
- [36] B.G. Rånby, J.F. Rabek, Photodegradation, Photo-oxidation, and Photo-stabilization of Polymers: Principles and Applications, John Wiley & Sons, New York, NY, 1975, (<https://books.google.co.uk/books?id=DEkQAQAIAAJ>).
- [37] J. Schafferhans, A. Baumann, A. Wagenpfahl, C. Deibel, V. Dyakonov, Oxygen doping of P3HT:PCBM blends: influence on trap states, charge carrier mobility and solar cell performance, *Org. Electron. Phys. Mater. Appl.* 11 (2010) 1693–1700, <http://dx.doi.org/10.1016/j.orgel.2010.07.016>.
- [38] S. Karuthedath, T. Sauermann, H.-J. Egelhaaf, R. Wannemacher, C.J. Brabec, L. Lüer, The effect of oxygen induced degradation on charge carrier dynamics in P3HT:PCBM and Si-PCPDTBT:PCBM thin films and solar cells, *J. Mater. Chem. A* 3 (2015) 3399–3408, <http://dx.doi.org/10.1039/C4TA06719C>.
- [39] X. Lemaire, Off-grid electrification with solar home systems: the experience of a fee-for-service concession in South Africa, *Energy Sustain. Dev.* 15 (2011) 277–283, <http://dx.doi.org/10.1016/j.esd.2011.07.005>.